An Analytical Tool to Evaluate Defect Thermodynamics of (La,Ba)$Fe_{1-x}M_xO_{3-\delta}$ Perovskites for Solid-Oxide Cell Applications

Yueh-Lin Lee
Senior Research Scientist, NETL Support Contractor

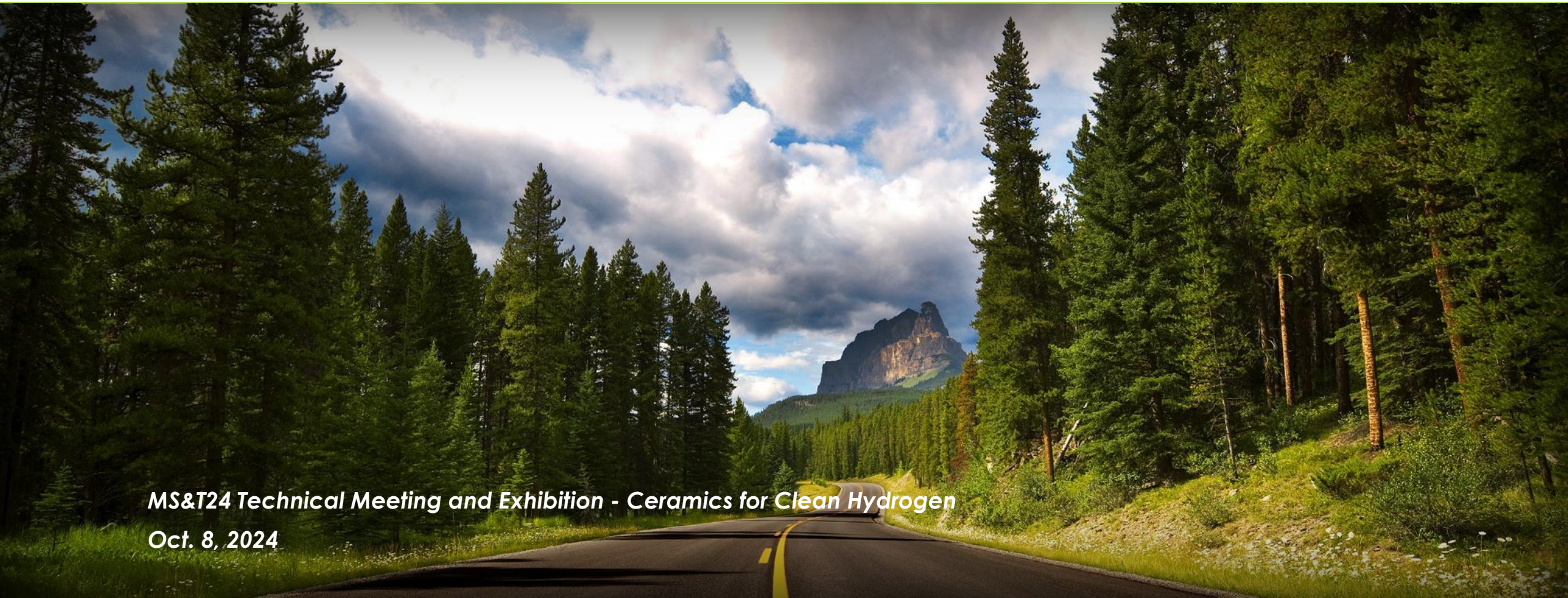

MS&T24 Technical Meeting and Exhibition - Ceramics for Clean Hydrogen

Oct. 8, 2024

Disclaimer

This project was funded by the United States Department of Energy, National Energy Technology Laboratory, in part, through a site support contract. Neither the United States Government nor any agency thereof, nor any of their employees, nor the support contractor, nor any of their employees, makes any warranty, express or implied, or assumes any legal liability or responsibility for the accuracy, completeness, or usefulness of any information, apparatus, product, or process disclosed, or represents that its use would not infringe privately owned rights. Reference herein to any specific commercial product, process, or service by trade name, trademark, manufacturer, or otherwise does not necessarily constitute or imply its endorsement, recommendation, or favoring by the United States Government or any agency thereof. The views and opinions of authors expressed herein do not necessarily state or reflect those of the United States Government or any agency thereof.

Authors and Contact Information

Yueh-Lin Lee[1,2]; Yuhua Duan[1]; Dan C. Sorescu[1]; Wissam A. Saidi[1]; Dane Morgan[3,5]; Thomas, Kalapos[1,2]; William T. Epting[4]; Gregory Hackett[3]; Harry Abernathy[3]

[1]National Energy Technology Laboratory, 626 Cochran Mill Road, Pittsburgh, PA 15236, USA

[2]NETL Support Contractor, 626 Cochran Mill Road, Pittsburgh, PA 15236, USA

[3]National Energy Technology Laboratory, 3610 Collins Ferry Road, Morgantown, WV 26505, USA

[4]National Energy Technology Laboratory, 1450 SW Queen Avenue, Albany, OR 97321, USA

[5]University of Wisconsin–Madison, 1509 University Avenue, Madison, WI 53706, USA

Introduction

- Utilization of proton-conducting materials has been adopted as a tactic to lower the operating temperature of the solid oxide cells (SOC) with improved efficiency and to mitigate degradation and cost issues occurring at high temperatures.
- $BaFeO_{3-\delta}$ and its alloy compounds are promising candidates as electrode materials for development of protonic conducting ceramic cells, due to their high proton conductivity at intermediate temperatures.
- Characterizing defect and transport properties of triple-conducting oxides remains a challenging task due to:
  - Complex coupling of protonic conductivity with electronic and oxygen-ion conductivities.
  - The need to determine the defect equilibria ($OH_O^{\bullet}$, charge, and $V_O^{\bullet\bullet}$) in response to the operating conditions.

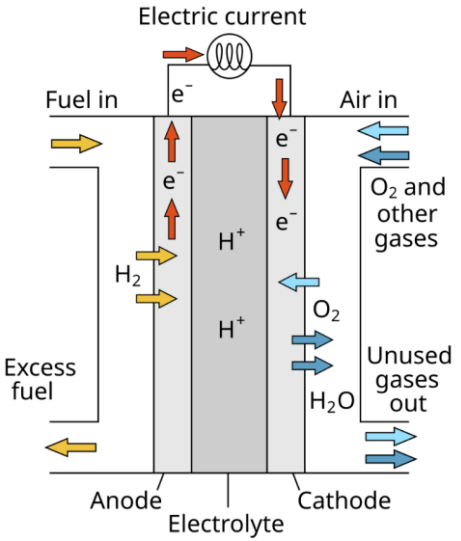

https://en.wikipedia.org/wiki/Protonic_ceramic_fuel_cell

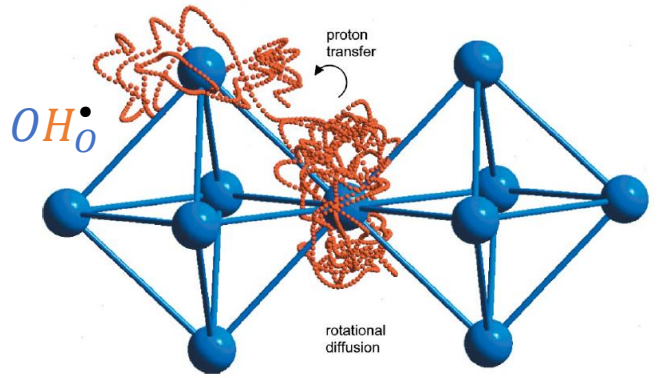

Kreuer, Annu. Rev. Mater. Res. 2003. 33:333–59.

Duan et al, Science, (2015) 349: 1321.
Merkle, Annu. Rev. Mater. Res., (2021) 51:461.
Duffy, J. Mater. Chem. A, (2023), 11, 8929.

Objectives and Defect Modeling Tools

- Recent studies identified δ dependence in defect energies (enthalpies) of hydration reaction and oxygen vacancy formation reaction (linear or nonlinear function forms)[1-3].
- Use density functional theory (DFT) calculations to correlate the electronic structure information to energetic and transport properties of materials and rationalize their influences on the defect thermodynamics.
- Conversion of $P(O_2)/P(H_2O)$ expressions to the $P(H_2)/P(H_2O)$ expressions is needed for understanding defect equilibria of oxide materials used in the fuel electrode applications.

Available Defect Modeling Tools at NETL

1. Defect Thermodynamic Model Tools for Proton and Oxide Conducting Electrolytes
   - **JOM**, (2022), 74, 4506.
   - **Physical Review Research**, (2021), 3, 013121.
2. Perovskite Defect Thermodynamic Model Tool for Triple Conducting Oxides
   - **ECS Transactions**, (2023) 111, (6) 1823-1838; Submitted to **JES (2024)** in July; under review.

[1]Sereda, Acta Materialia, 2019, 162, 33-45.
[2]*Hoedl, J. Phys. Chem. C 2020, 124, 11780.*
[3]*Millican, Chem. Mater.* 2022, 34, 2, 510.

1. Defect Thermodynamics and Transport Properties of Proton Conducting Electrolyte $BaZr_{1-x}Y_xO_{3-\delta}$ ($x \leq 0.1$)

NATIONAL ENERGY TECHNOLOGY LABORATORY

Electron-poor oxide material

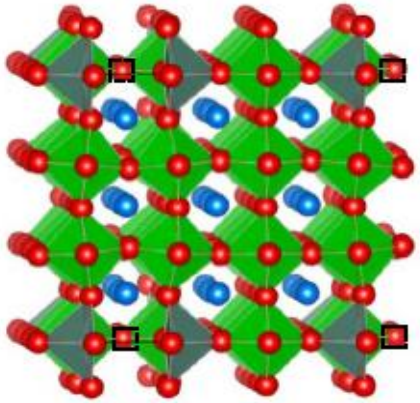

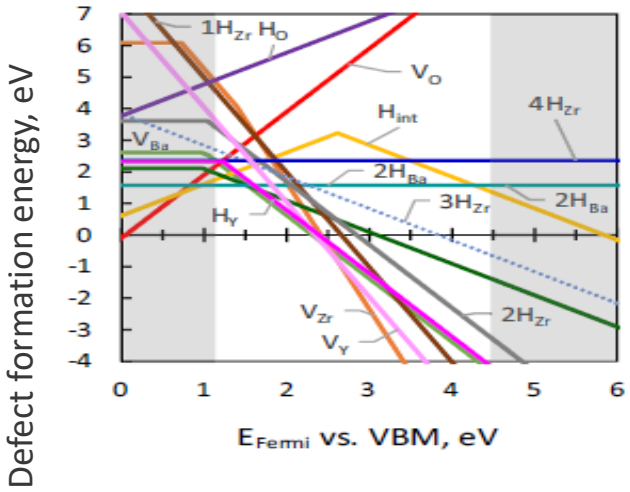

T=1000K

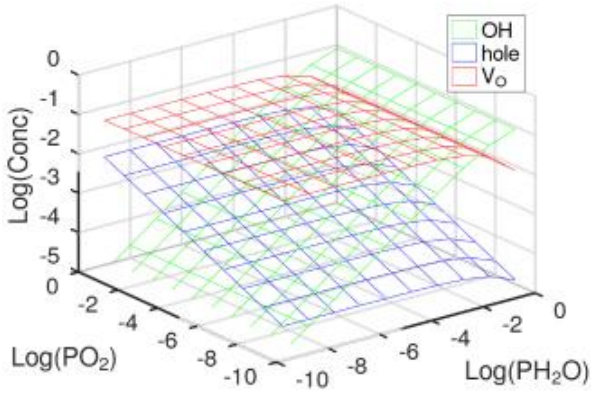

T=800K

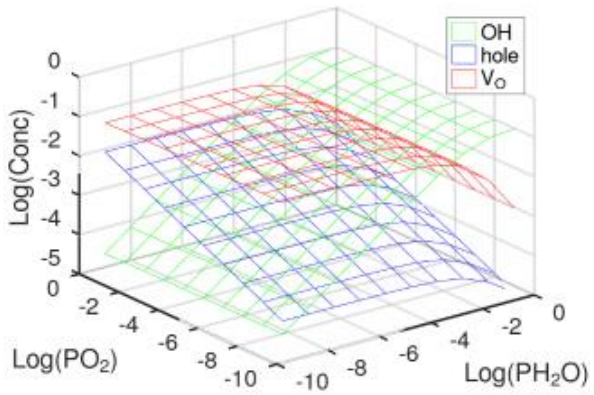

vs. $P(O_2)$

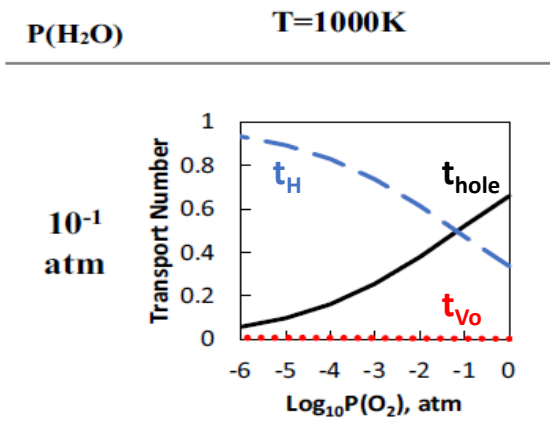

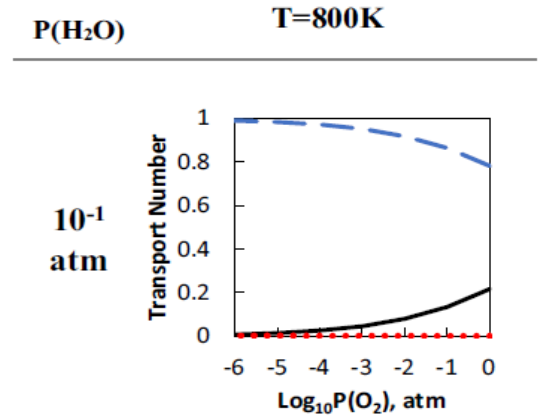

vs. $P(H_2)$

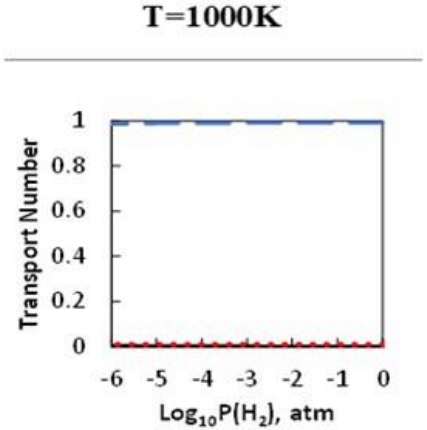

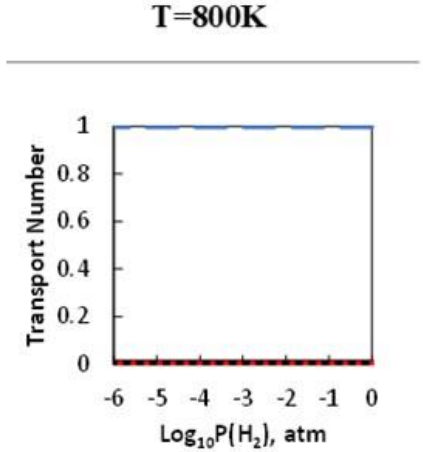

JOM, 74, 4506–4526 (2022).

2. Defect Thermodynamics and Transport Properties of Triple Conducting Electrode $Ba_{1-x}La_xFe_{1-y}M_yO_{3-\delta}$ (M= Y, Zr)

NATIONAL ENERGY TECHNOLOGY LABORATORY

Electron-rich oxide material: $Ba_{0.95}La_{0.05}Fe_{0.9}O_{3-\delta}$

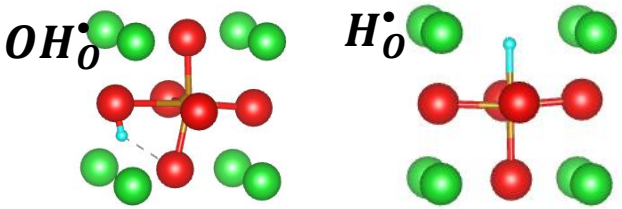

- Generate Brouwer diagrams of $Ba_{0.95}La_{0.05}Fe_{0.9}O_{3-\delta}$ in a range of T and $P(O_2)/P(H_2O)$ or $P(H_2)/P(H_2O)$ conditions.
- Methodology extended to include the hydride ($H_O^{\bullet}$) defect formation energies and entropies into the model, allowing to examine defect equilibria under reducing conditions.

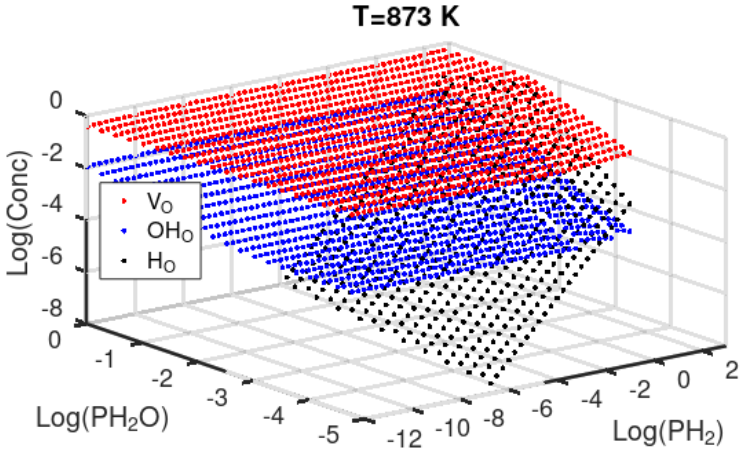

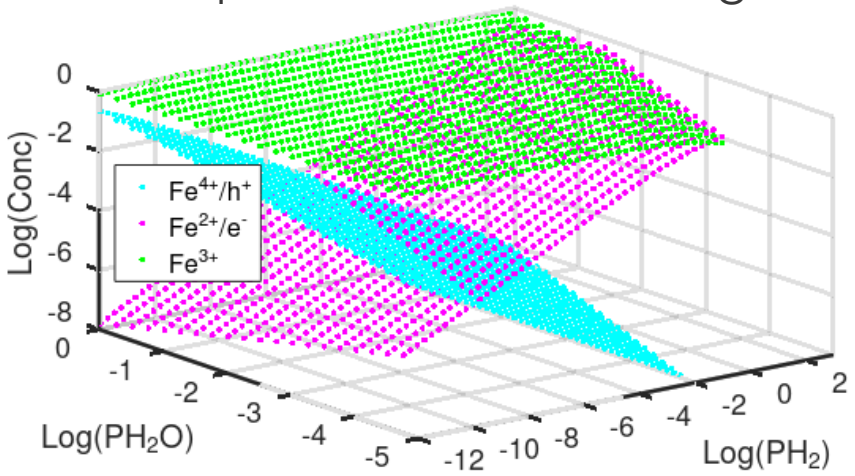

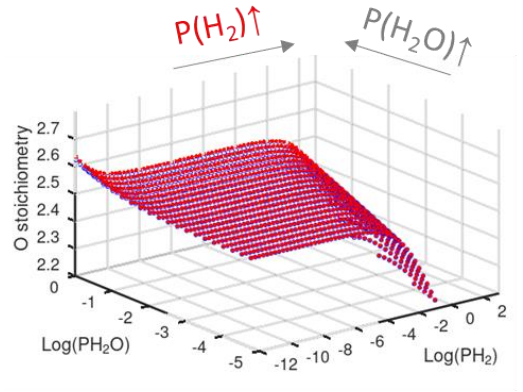

O stoichiometry

Developed GNU-Octave scripts to model (La,Ba)$Fe_{1-x}M_xO_{3-\delta}$ defect thermodynamics
Available at NETL-EDX: https://edx.netl.doe.gov/dataset/triple_conducting_perovskite_defect_model

JES (2024), under review.

Non-Rigid Band Defect Behavior

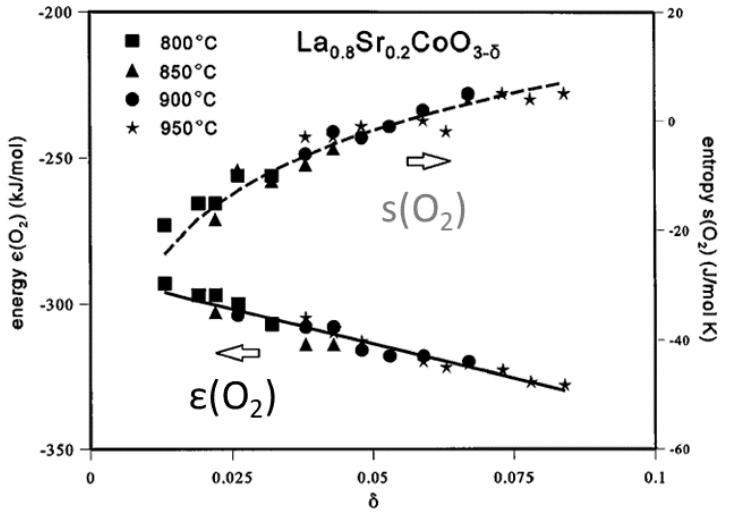

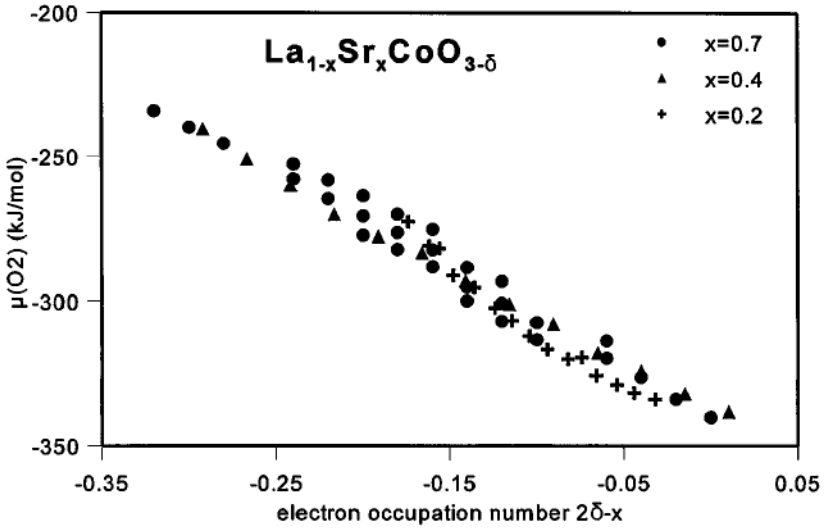

Lankhorst, Phys. Rev. Lett., 1996, 77, 2989; JSSC, 1997, 133, 555-567.

$$\varepsilon_{O_2}^{oxide} = E_{ox} - \frac{4(2[V_O^{\cdot\cdot}] - x)}{g(\varepsilon_F)}$$

$g(\varepsilon_F)$: Electronic Density of States

VS.

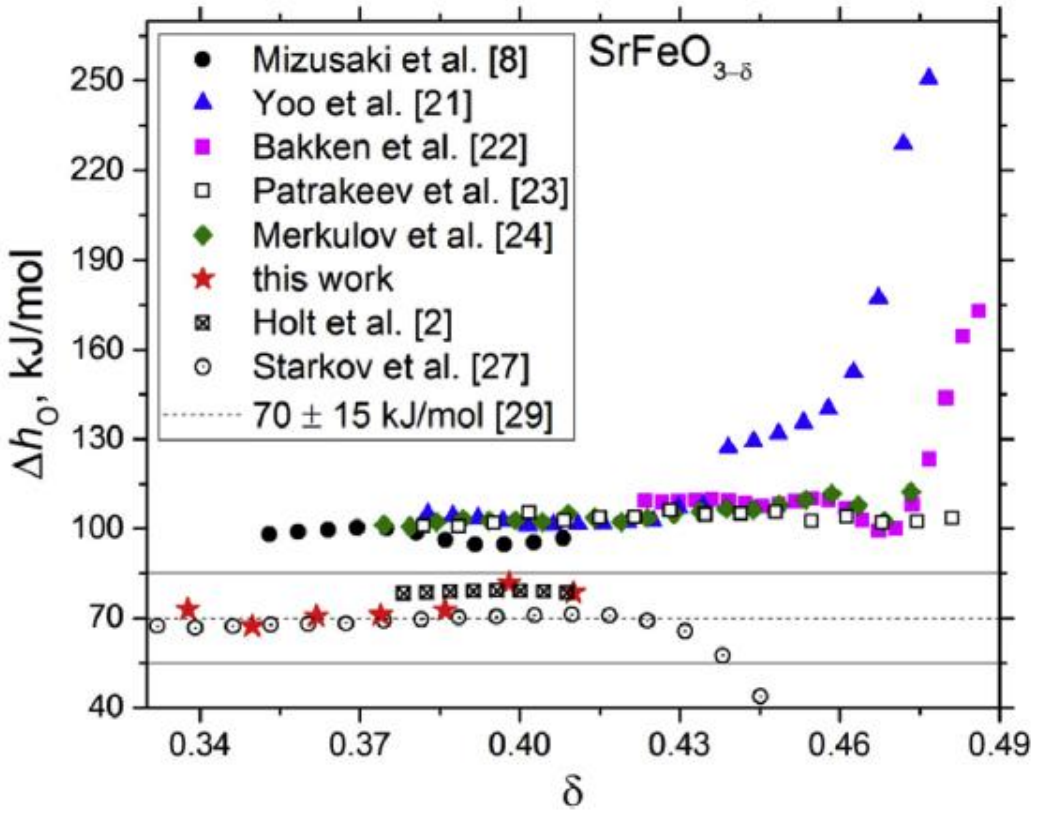

- Non-linear $\varepsilon(O_2)$ or Δh_O needs alternative description beyond the rigid band model.

Sereda, Acta Materialia, 2019, 162, 33-45.

Generalized Defect Model for (La,A)(M,B)$O_{3-\delta}$ Perovskites

- A range of physically possible $[V_O^{\bullet\bullet}]$ values are selected to reversely solve the defect model and to obtain the corresponding P(O_2).
- Can include nonlinear or higher order δ terms (quadratic, cubic,….) for the defect reaction energies/entropies.

TABLE II. Small polaron (SP) and large polaron (LP) expressions of the defect thermodynamic model equations used for solving the unknown variables (as listed in TABLE I) as a function of temperature.

Label	Model Expression	Equations	
A-site conservation	SP, LP	$[Ba_A^{'}] + [La_A^{x}] = 1$	[II.1]
B-site conservation	SP	$[Fe_B^{\bullet}]+[Fe_B^{'}] + [Fe_B^{x}] + [M_B^{q}] = 1$	[II.2a]
	LP	$[Fe_B] + [M_B^{q}] = 1$	[II.2b]
O-site conservation	SP, LP	$[OH_O^{\bullet}] + [V_O^{\bullet\bullet}] + [O_O^{x}] = 3$	[II.3]
Charge neutrality	SP	$[Fe_B^{\bullet}] + 2[V_O^{\bullet\bullet}] + [OH_O^{\bullet}] + q \bullet [M^q] - [Fe_B^{'}] - [Ba_A^{'}] = 0$	[II.4a]
	LP	$[h^{\bullet}] + 2[V_O^{\bullet\bullet}] + [OH_O^{\bullet}] + q \bullet [M^q] - [e^{'}] - [Ba_A^{'}] = 0$	[II.4b]

O vacancy formation	SP	$2Fe_B^{\bullet} + O_O^{x} \leftrightarrow 2Fe_B^{x} + V_O^{\bullet\bullet} + \frac{1}{2}O_2$ $K_{O\,vac} = \exp\left(\frac{-\Delta E_{O\,vac}(\delta) + T\Delta S_{O\,vac}(\delta)}{k_b T}\right) = \frac{[Fe_B^{x}]^2 \cdot [V_O^{\bullet\bullet}] \cdot P(O_2)^{0.5}}{[Fe_B^{\bullet}]^2 \cdot [O_O^{x}]}$	[II.5a]
	LP	$2h_{\square}^{\bullet} + O_O^{x} \leftrightarrow V_O^{\bullet\bullet} + \frac{1}{2}O_2$ $K_{O\,vac} = \exp\left(\frac{-\Delta E_{O\,vac}(\delta) + T\Delta S_{O\,vac}(\delta)}{k_b T}\right) = \frac{[V_O^{\bullet\bullet}] \cdot P(O_2)^{0.5}}{[h^{\bullet}]^2 \cdot [O_O^{x}]}$	[II.5b]
Charge disproportion reaction	SP	$2Fe_B^{x} \leftrightarrow Fe_B^{\bullet} + Fe_B^{'}$ $K_{chg\,disp} = \exp\left(\frac{-\Delta E_{chg\,disp}(\delta) + T\Delta S_{chg\,disp}(\delta)}{k_b T}\right) = \frac{[Fe_B^{\bullet}] \cdot [Fe_B^{'}]}{[Fe_B^{x}]^2}$	[II.6a]
	LP	$nil \leftrightarrow h_{\square}^{\bullet} + e_{\square}^{'}$ $K_{chg\,disp} = \exp\left(\frac{-\Delta E_{chg\,disp}(\delta) + T\Delta S_{chg\,disp}(\delta)}{k_b T}\right) = [h^{\bullet}] \cdot [e^{'}]$	[II.6b]
Hydration reaction	SP, LP	$H_2O + V_O^{\bullet\bullet} + O_O^{x} \leftrightarrow 2OH_O^{\bullet}$ $K_{Hyd} = \exp\left(\frac{-\Delta E_{Hyd}(\delta) + T\Delta S_{Hyd}(\delta)}{k_b T}\right) = \frac{[OH_O^{\bullet}]^2}{P(H_2O) \cdot [V_O^{\bullet\bullet}] \cdot [O_O^{x}]}$	[II.7]
Hydride formation	SP	$\frac{1}{2}H_2 + V_O^{\bullet\bullet} + Fe_B^{'} \leftrightarrow H_O^{\bullet} + Fe_B^{x}$ or $\frac{1}{2}(H_2O - \frac{1}{2}O_2) + V_O^{\bullet\bullet} + Fe_B^{'} \leftrightarrow H_O^{\bullet} + Fe_B^{x}$ $K_{H^-} = \exp\left(\frac{-\Delta E_{H^-}(\delta) + T\Delta S_{H^-}(\delta)}{k_b T}\right)$ $= \frac{[Fe_B^{x}] \cdot [H_O^{\bullet}]}{[Fe_B^{'}] \cdot [V_O^{\bullet\bullet}] \cdot P(H_2)^{0.5}}$ or $= \frac{[Fe_B^{x}] \cdot [H_O^{\bullet}] \cdot P(O_2)^{0.25}}{[Fe_B^{'}] \cdot [V_O^{\bullet\bullet}] \cdot P(H_2O)^{0.5}}$	[II.8a]
	LP	$\frac{1}{2}H_2 + V_O^{\bullet\bullet} + e_{\square}^{'} \leftrightarrow H_O^{\bullet}$ or $\frac{1}{2}(H_2O - \frac{1}{2}O_2) + V_O^{\bullet\bullet} + e_{\square}^{'} \leftrightarrow H_O^{\bullet}$ $K_{H^-} = \exp\left(\frac{-\Delta E_{H^-}(\delta) + T\Delta S_{H^-}(\delta)}{k_b T}\right)$ $= \frac{[H_O^{\bullet}]}{[e_{\square}^{'}] \cdot [V_O^{\bullet\bullet}] \cdot P(H_2)^{0.5}}$ or $= \frac{[H_O^{\bullet}] \cdot P(O_2)^{0.25}}{[e_{\square}^{'}] \cdot [V_O^{\bullet\bullet}] \cdot P(H_2O)^{0.5}}$	[II.8b]

JES (2024), under review.

Defect Chemistry of $SrFe_{1-x}Sn_xO_{3-\delta}$

Apply the model to describe the experimental results reported in the literature.

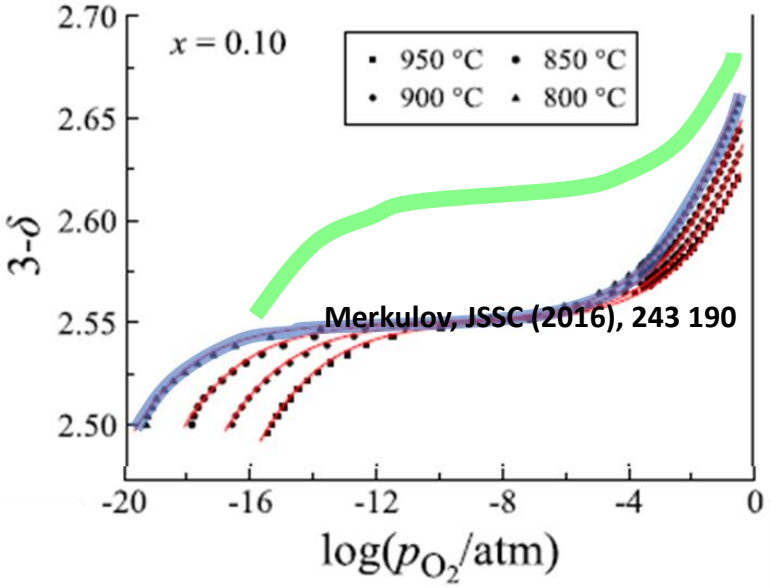

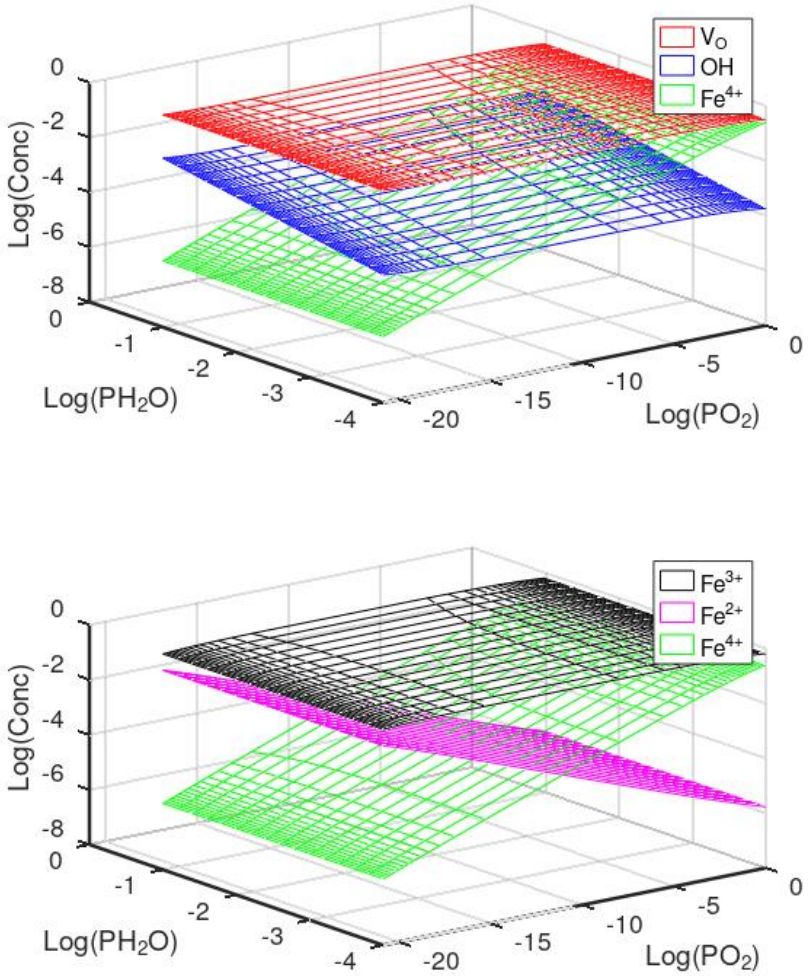

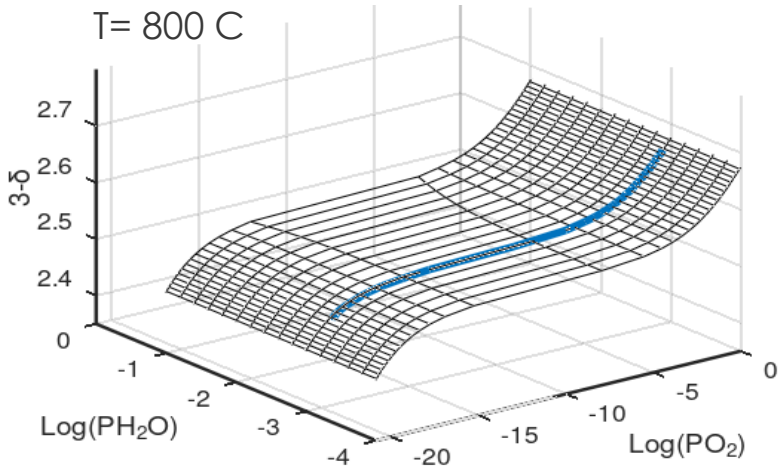

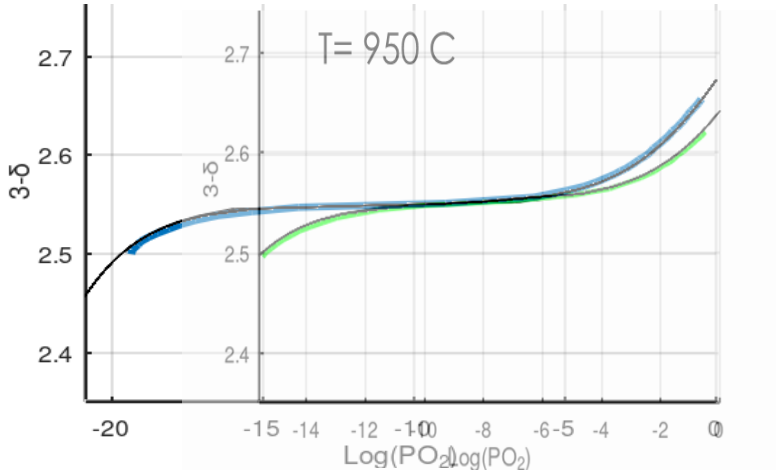

- Provide concentration information of $V_O^{\bullet\bullet}$, $OH_O^{\bullet}$, Fe^{2+}, Fe^{3+}, and Fe^{4+} in a range of $P(O_2)$ and $P(H_2O)$.

Reaction Energetics for Modeling $BaFe_{0.9}Y_{0.1}O_{3-\delta}$

Yttria Substituted $BaFeO_{3-\delta}$

Chemical reaction equilibrium constants can be determined either from DFT or experiments:

$$K_{rxn} = exp(-\frac{\Delta G_{rxn}}{k_b T}) = exp(-\frac{\Delta H_{rxn} - T\Delta S_{rxn}}{k_b T}) = \frac{\prod_j B_{p\_j}^{n_{p\_j}}}{\prod_i A_{r\_i}^{m_{r\_i}}}$$

$$\Delta H_{rxn}(C(B_p), T, \ldots.): \Delta H_{rxn} = \Delta E_{DFT} + \Upsilon \bullet C(V_O^{\bullet\bullet}) + \ldots.$$

e.g., O vacancy formation reaction:

$$K_{O\ vac} = \exp\left(\frac{-\Delta H_{O\ vac} + T\Delta S_{O\ vac}}{k_b T}\right)$$

$$= \exp\left(\frac{-(\Delta E_{O\ vac} + \Upsilon \bullet \delta + \cdots.) + T\Delta S_{O\ vac}}{k_b T}\right) = \frac{[Fe_B^x]^2 [V_O^{\bullet\bullet}] \cdot P(O_2)^{0.5}}{[Fe_B^{\bullet}]^2 \cdot O_O^x}$$

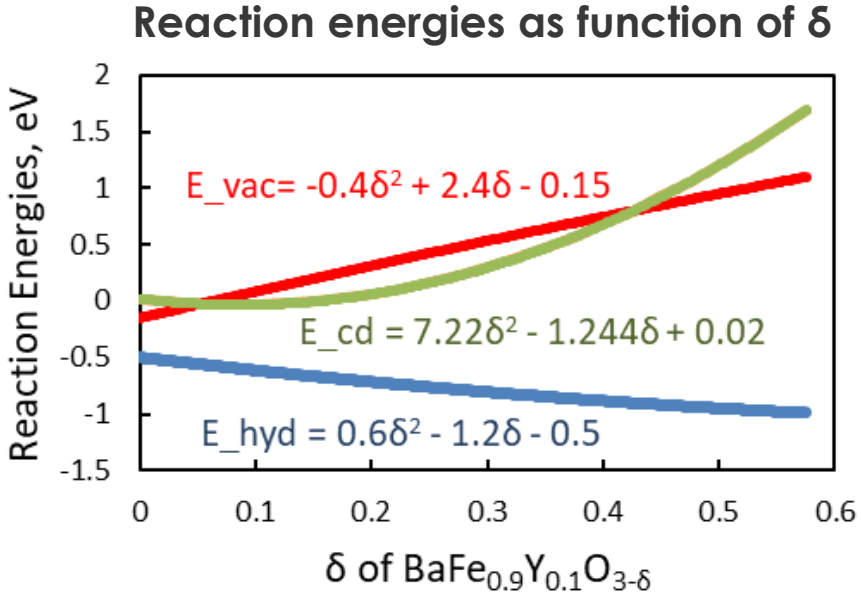

E_{vac}: O vac. formation reaction E
E_{hyd}: hydration reaction E
E_{CD} : charge disproportionation E

ECS Transactions, (2023) 111, (6) 1823-1838.

Defect Chemistry of $BaFe_{0.9}Y_{0.1}O_{3-\delta}$ at T=800 K

(a) $BaFe_{0.9}Y_{0.1}O_{3-\delta}$ at T=600 K

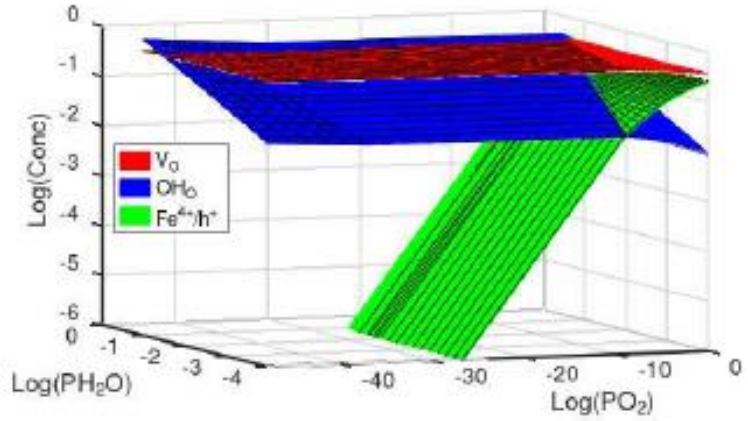

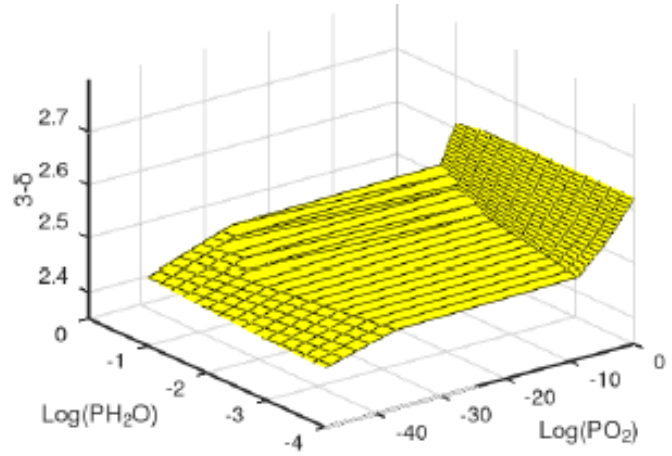

O stoichiometry.

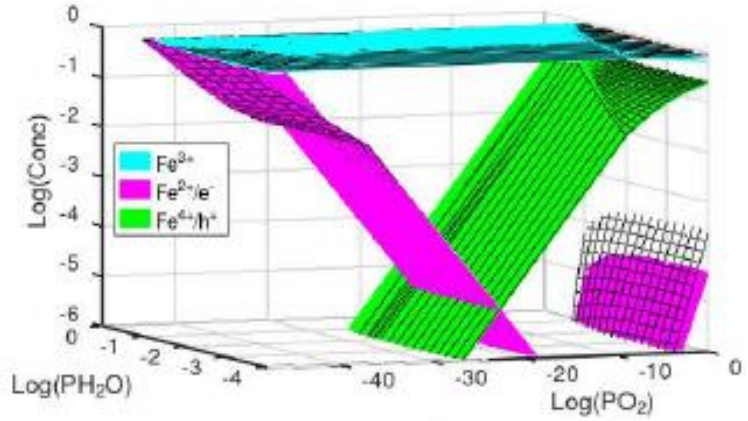

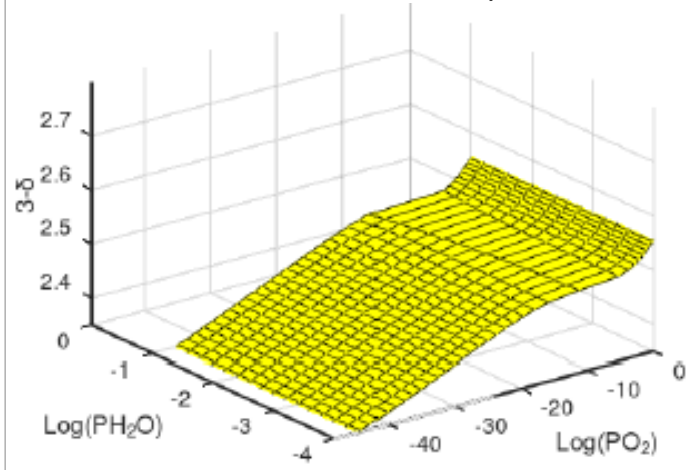

O stoichiometry.

(b) $BaFe_{0.9}Y_{0.1}O_{3-\delta}$ at T=1000 K

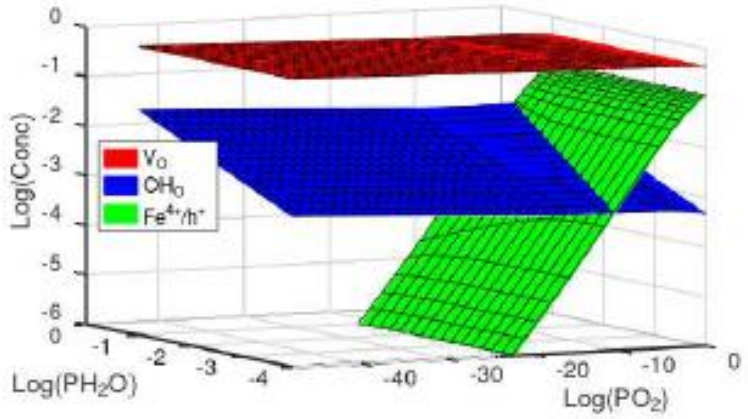

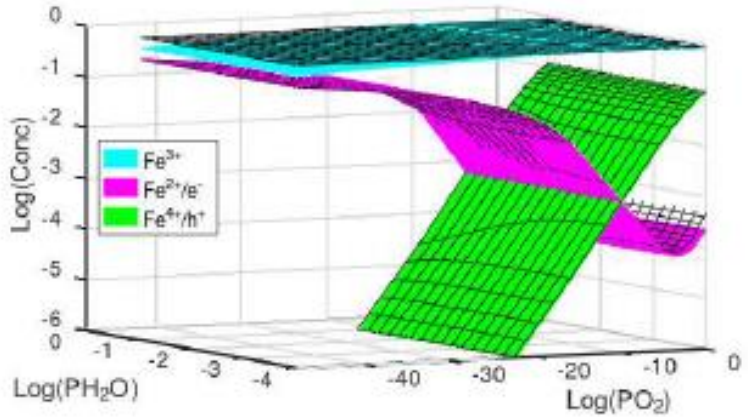

ECS Transactions, (2023) 111, (6) 1823-1838.

Distinct Gas Pressure Dependences: $P(H_2)/P(H_2O)$ vs. $P(O_2)/P(H_2O)$

Brouwer Diagrams of $Ba_{0.95}La_{0.05}FeO_{3-\delta}$ at T = 873 K

$P(O_2)/P(H_2O)$ description

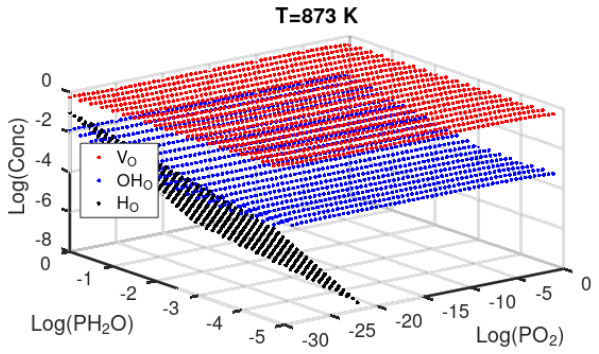

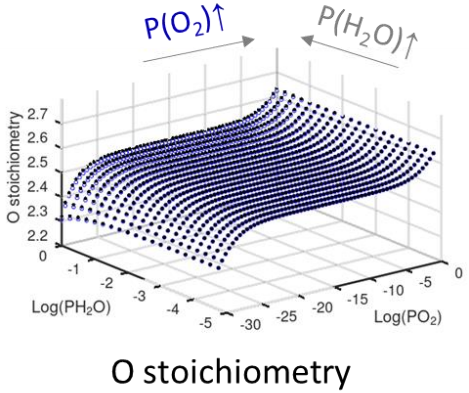

O stoichiometry

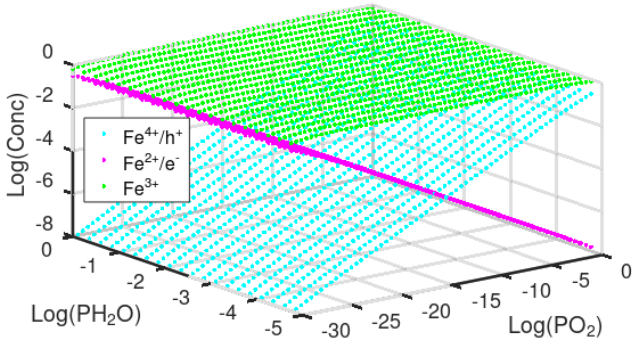

- $[H_O^{\bullet}]$ more prominent when $P(O_2)$ is 10^{-15} atm or lower.
- Increasing $P(H_2O)$ increases $[H_O^{\bullet}]$ at lower $P(O_2)$.
- Crossover of $[H_O^{\bullet}]$ vs. $[OH_O^{\bullet}]$ is predicted to occur at $P(O_2)$ approximately equal to 10^{-21} atm at $P(H_2O)$ = 1 atm.

$P(H_2)/P(H_2O)$ description

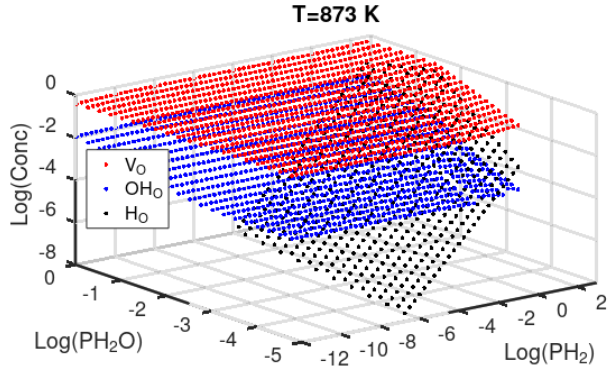

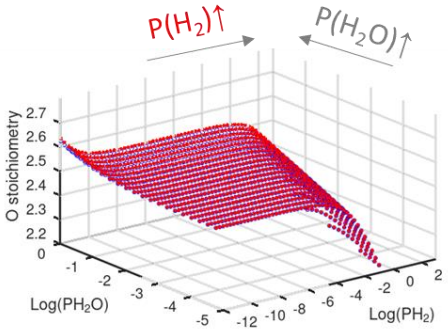

O stoichiometry

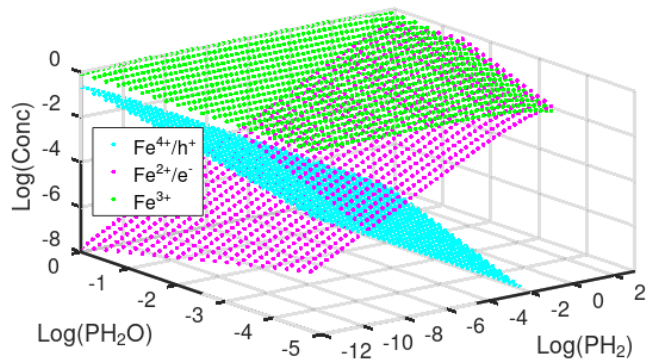

- Reversed trend in defect concentrations vs. $P(H_2)/P(H_2O)$ as compared with those vs. $P(O_2)/P(H_2O)$.

JES (2024), under review.

Distinct Gas Pressure Dependences (Both in Reducing Conditions)

Oxygen Poor or Low $P(O_2)$ vs. Hydrogen Rich or High $P(H_2)$ Conditions

The results highlight conversion of the Brouwer diagrams from the $P(O_2)/P(H_2O)$ expression to the $P(H_2)/P(H_2O)$ expression, which experimentally are more accessible in the later scenario, for interpretation of the gas pressure and temperature dependences of the defect chemistry.

$P(H_2)$ = 0.21 atm

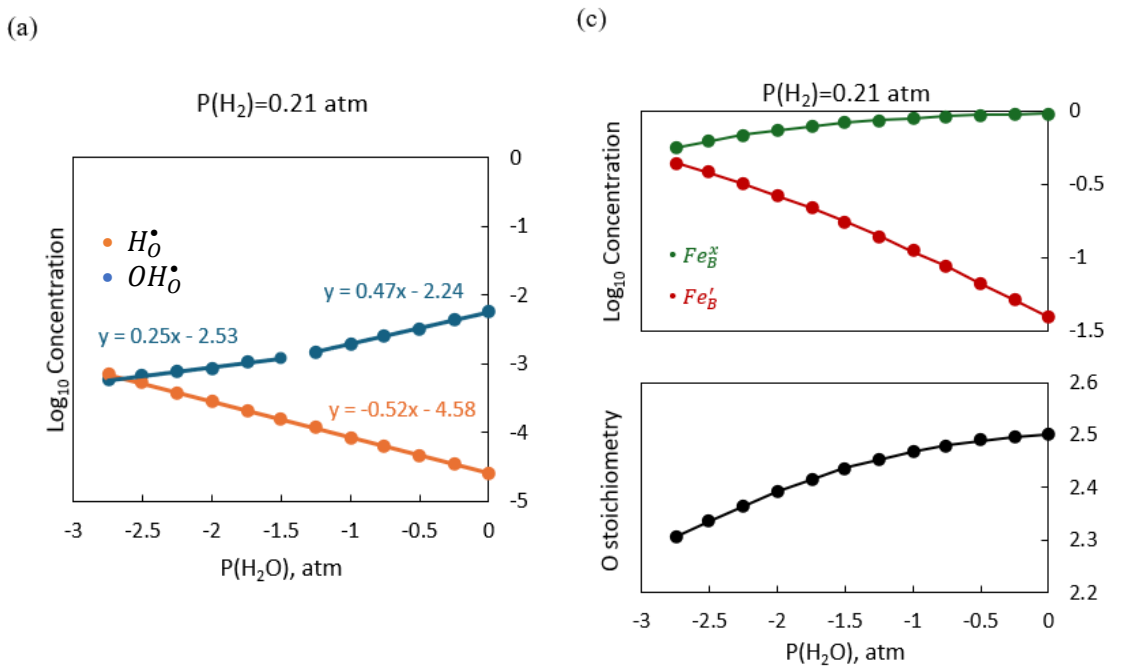

$P(O_2)$ = 10^{-23} atm

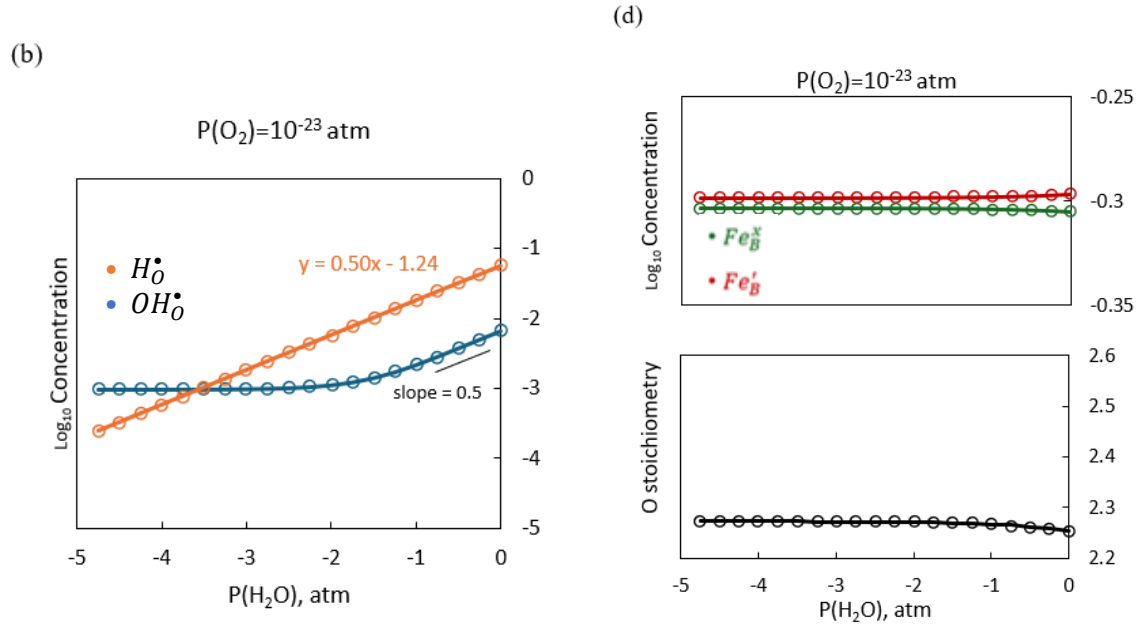

JES (2024), under review.

Distinct Gas Pressure Dependences: $P(H_2)/P(H_2O)$ vs. $P(O_2)/P(H_2O)$

(a) $P(H_2)$ = 0.21 atm

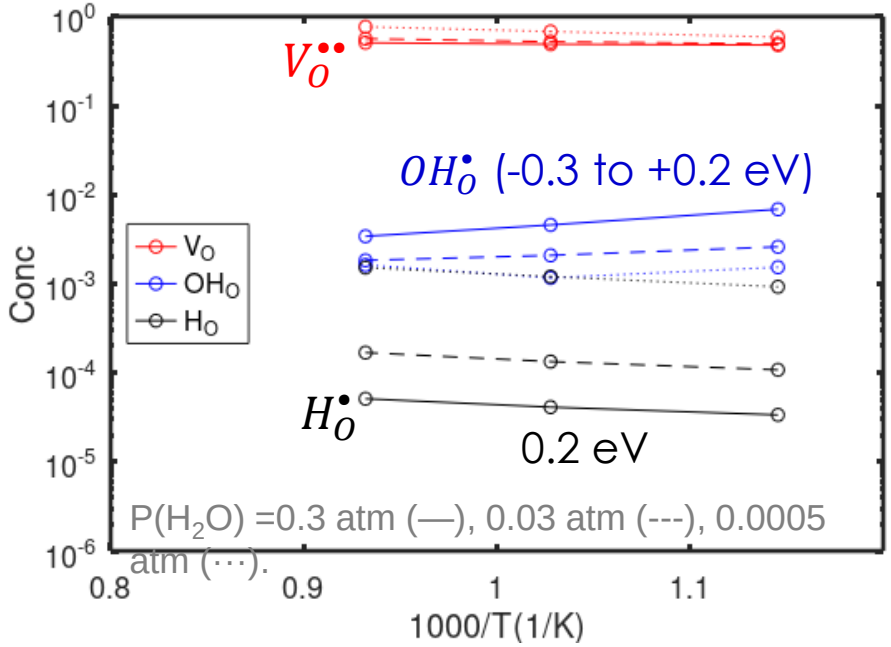

(b) $P(O_2)$ = 10^{-23} atm

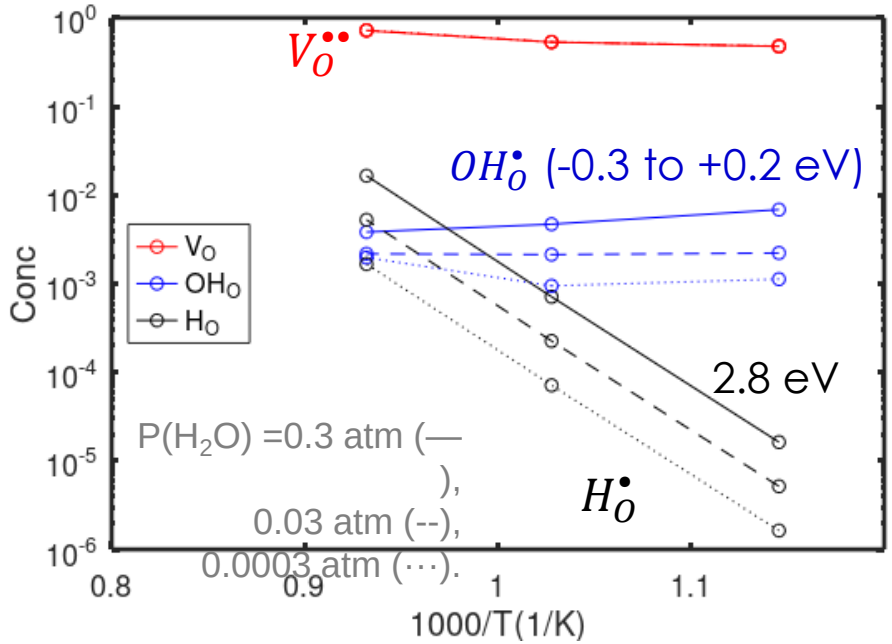

For the $OH_O^{\bullet}$ proton defect (blue lines):

- Apparent formation energies within the range of **-0.3 to +0.2** eV.

For the $H_O^{\bullet}$ hydride defect (black lines):

- Apparent formation energies of **0.2 eV** under **$P(H_2)$=0.21 atm** vs. **2.8 eV** under **$P(O_2)$ = 10^{-23} atm.**

JES (2024), under review.

Summary

- A generalized defect thermodynamic modeling tool was developed for triple conducting $(Ba_{1-x}La_x)Fe_{1-y}M_yO_{3-\delta}$ perovskite which can be found here:
  - https://edx.netl.doe.gov/dataset/triple_conducting_perovskite_defect_model
- The developed defect model is able to go beyond the rigid-band type defect model systems.
  - Non-rigid band defect behavior is due to δ dependent electronic/magnetic structures.
- Hydrogen defect species are incorporated into the model for a wide range of $P(H_2)/P(H_2O)$ or $P(O_2)/P(H_2O)$ conditions.
  - Included in the hydride species $H_O^{\bullet}$ for the reduced (e.g., fuel electrode) conditions.
  - Identified distinct temperature and gas pressure dependences for the defect species between the $P(H_2)/P(H_2O)$ and $P(O_2)/P(H_2O)$ expressions in reduced conditions.
- This computational capability facilitates understanding of the bulk defect thermodynamics and its role in performance improvement and is beneficial to computational material screening of triple conducting perovskites for the SOC applications.

Acknowledgments

This work was performed in support of the U.S. Department of Energy's (DOE) Office of Fossil Energy and Carbon Management's Solid Oxide Fuel Cell Research Program and executed through the National Energy Technology Laboratory (NETL) Research & Innovation Center's Solid Oxide Fuel Cell Multi Year Research Plan.

NETL RESOURCES

VISIT US AT: **www.NETL.DOE.gov**

@NETL_DOE

@NETL_DOE

@NationalEnergyTechnologyLaboratory

CONTACT:

Yueh-Lin Lee
Yueh-Lin.Lee@netl.doe.gov

Abstract

A modeling tool of the defect thermodynamics of (La,Ba)$Fe_{1-x}M_xO_{3-\delta}$ perovskites which includes energetic information about oxygen vacancy formation, hydration, hydride formation, and charge disproportionation reactions has been developed[1]. This tool incorporates defect energies and entropies expressed as sixth order polynomial functions to allow refinements of the defect reaction equilibrium constants in the thermodynamic analysis. Calculation of (La,Ba)$Fe_{1-x}M_xO_{3-\delta}$ Brouwer diagrams as a function of pO_2/pH_2O and pH_2/H_2O in a range of temperatures of interest is facilitated by this modeling tool. The results obtained can provide direct guidance on how the electronic and ionic defect concentrations of the triple conducting perovskite materials can be used to optimize performance of solid oxide cells for energy applications. The impact of magnetic and electronic structures of the perovskites on the defect reaction energies and entropies as obtained from density function theory modeling and the role played by hydride defect species will also be discussed.

[1]https://edx.netl.doe.gov/dataset/triple_conducting_perovskite_defect_model

Workflow of the Defect Model Solver

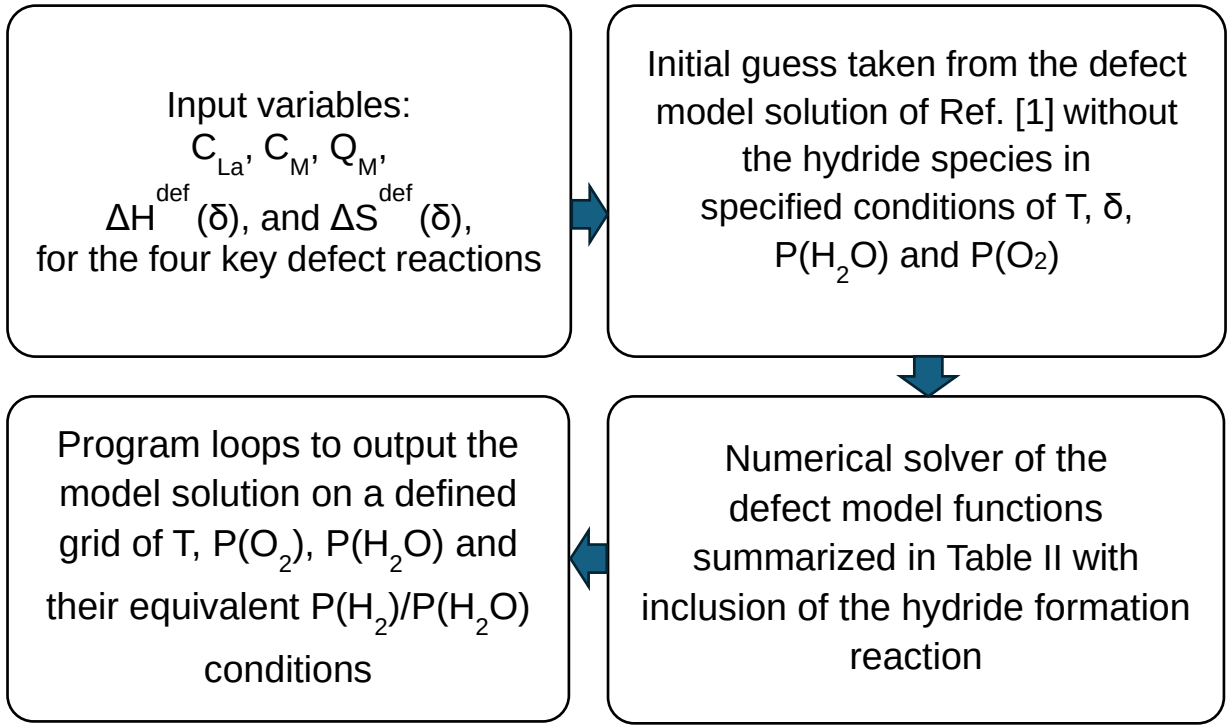

TABLE II. Small polaron (SP) and large polaron (LP) expressions of the defect thermodynamic model equations used for solving the unknown variables (as listed in TABLE I) as a function of temperature.

Label	Model Expression	Equations	
A-site conservation	SP, LP	$[Ba'_A] + [La^{\bullet}_A] = 1$	[II.1]
B-site conservation	SP	$[Fe^{\bullet}_B]+[Fe'_B] + [Fe^{x}_B] + [M^{x}_B] = 1$	[II.2a]
	LP	$[Fe_B] + [M^{x}_B] = 1$	[II.2b]
O-site conservation	SP, LP	$[OH^{\bullet}_O] + [V^{\bullet\bullet}_O] + [O^{x}_O] = 3$	[II.3]
Charge neutrality	SP	$[Fe^{\bullet}_B] + 2[V^{\bullet\bullet}_O] + [OH^{\bullet}_O] + q \bullet [M^{q}] - [Fe'_B] - [Ba'_A] = 0$	[II.4a]
	LP	$[h^{\bullet}] + 2[V^{\bullet\bullet}_O] + [OH^{\bullet}_O] + q \bullet [M^{q}] - [e'] - [Ba'_A] = 0$	[II.4b]
O vacancy formation	SP	$2Fe^{\bullet}_B + O^{x}_O \leftrightarrow 2Fe^{x}_B + V^{\bullet\bullet}_O + \frac{1}{2}O_2$ $K_{O\,vac} = \exp\left(\frac{-\Delta E_{O\,vac}(\delta) + T\Delta S_{O\,vac}(\delta)}{k_b T}\right) = \frac{[Fe^{x}_B]^2 \cdot [V^{\bullet\bullet}_O] \cdot P(O_2)^{0.5}}{[Fe^{\bullet}_B]^2 \cdot [O^{x}_O]}$	[II.5a]
	LP	$2h^{\bullet}_{\square} + O^{x}_O \leftrightarrow V^{\bullet\bullet}_O + \frac{1}{2}O_2$ $K_{O\,vac} = \exp\left(\frac{-\Delta E_{O\,vac}(\delta) + T\Delta S_{O\,vac}(\delta)}{k_b T}\right) = \frac{[V^{\bullet\bullet}_O] \cdot P(O_2)^{0.5}}{[h^{\bullet}]^2 \cdot [O^{x}_O]}$	[II.5b]
Charge disproportion reaction	SP	$2Fe^{x}_B \leftrightarrow Fe^{\bullet}_B + Fe'_B$ $K_{chg\,disp} = \exp\left(\frac{-\Delta E_{chg\,disp}(\delta) + T\Delta S_{chg\,disp}(\delta)}{k_b T}\right) = \frac{[Fe^{\bullet}_B] \cdot [Fe'_B]}{[Fe^{x}_B]^2}$	[II.6a]
	LP	$n\vec{\imath} \leftrightarrow h^{\bullet}_{\square} + e_{\square}$ $K_{chg\,disp} = \exp\left(\frac{-\Delta E_{chg\,disp}(\delta) + T\Delta S_{chg\,disp}(\delta)}{k_b T}\right) = [h^{\bullet}] \cdot [e']$	[II.6b]
Hydration reaction	SP, LP	$H_2O + V^{\bullet\bullet}_O + O^{x}_O \leftrightarrow 2OH^{\bullet}_O$ $K_{hyd} = \exp\left(\frac{-\Delta E_{hyd}(\delta) + T\Delta S_{hyd}(\delta)}{k_b T}\right) = \frac{[OH^{\bullet}_O]^2}{P(H_2O) \cdot [V^{\bullet\bullet}_O] \cdot [O^{x}_O]}$	[II.7]
Hydride formation	SP	$\frac{1}{2}H_2 + V^{\bullet\bullet}_O + Fe^{\bullet}_B \leftrightarrow H^{\bullet}_O + Fe^{x}_B$ or $\frac{1}{2}(H_2O - \frac{1}{2}O_2) + V^{\bullet\bullet}_O + Fe^{\bullet}_B \leftrightarrow H^{\bullet}_O + Fe^{x}_B$ $K_{H^-} = \exp\left(\frac{-\Delta E_{H^-}(\delta) + T\Delta S_{H^-}(\delta)}{k_b T}\right)$ $= \frac{[Fe^{x}_B]\cdot[H^{\bullet}_O]}{[Fe^{\bullet}_B]\cdot[V^{\bullet\bullet}_O]\cdot P(H_2)^{0.5}}$ or $= \frac{[Fe^{x}_B]\cdot[H^{\bullet}_O]\cdot P(O_2)^{0.25}}{[Fe^{\bullet}_B]\cdot[V^{\bullet\bullet}_O]\cdot P(H_2O)^{0.5}}$	[II.8a]
	LP	$\frac{1}{2}H_2 + V^{\bullet\bullet}_O + e_{\square} \leftrightarrow H^{\bullet}_O$ or $\frac{1}{2}(H_2O - \frac{1}{2}O_2) + V^{\bullet\bullet}_O + e_{\square} \leftrightarrow H^{\bullet}_O$ $K_{H^-} = \exp\left(\frac{-\Delta E_{H^-}(\delta) + T\Delta S_{H^-}(\delta)}{k_b T}\right)$ $= \frac{[H^{\bullet}_O]}{[e'_{\square}]\cdot[V^{\bullet\bullet}_O]\cdot P(H_2)^{0.5}}$ or $= \frac{[H^{\bullet}_O]\cdot P(O_2)^{0.25}}{[e'_{\square}]\cdot[V^{\bullet\bullet}_O]\cdot P(H_2O)^{0.5}}$	[II.8b]

Workflow of the developed defect model solver that includes the hydride defect formation reaction. The defect model equations are summarized in Table II. C_{La} and C_M are concentrations of La and M (M= non-transition metal) substitutions at the A-site and B-site of $BaFeO_{3-\delta}$, respectively.

[1] ECS Transactions, 111 (6) 1823 (2023).

Rigid-Band Type Defect Behavior for Perovskite Oxides

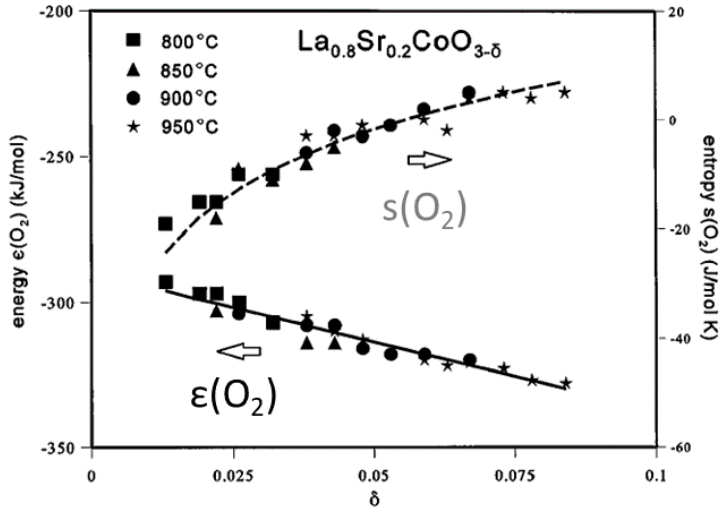

$$\varepsilon_{O_2}^{oxide} = E_{ox} - \frac{4(2[V_O^{\cdot\cdot}] - x)}{g(\varepsilon_F)}$$

$g(\varepsilon_F)$: Electronic Density of States

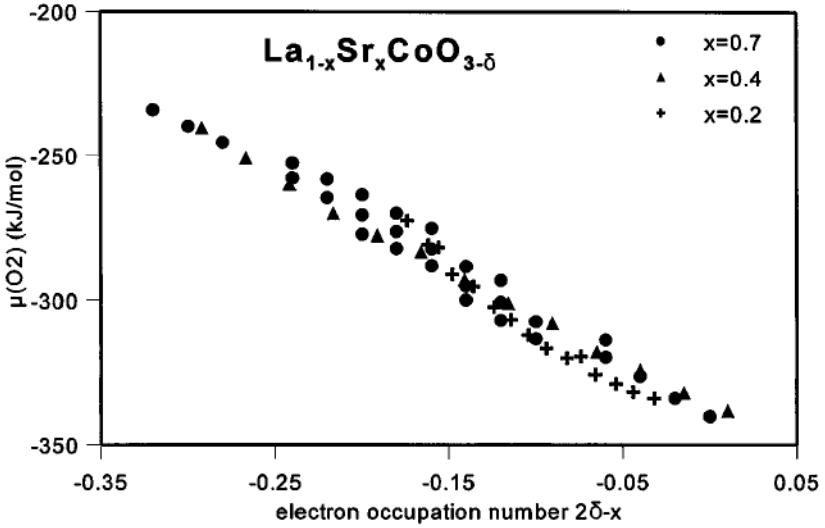

Lankhorst, Phys. Rev. Lett., 1996, 77, 2989; JSSC, 1997, 133, 555-567.

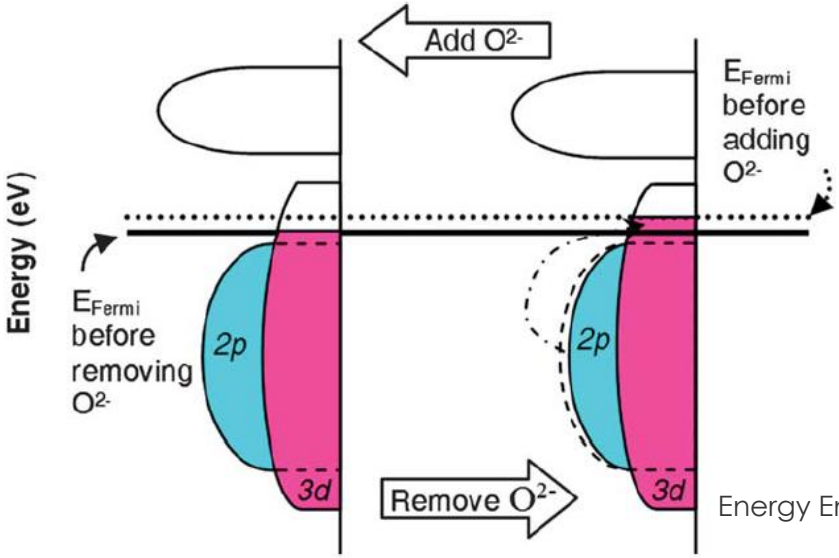

Energy Environ. Sci., 2011, 4, 3966.

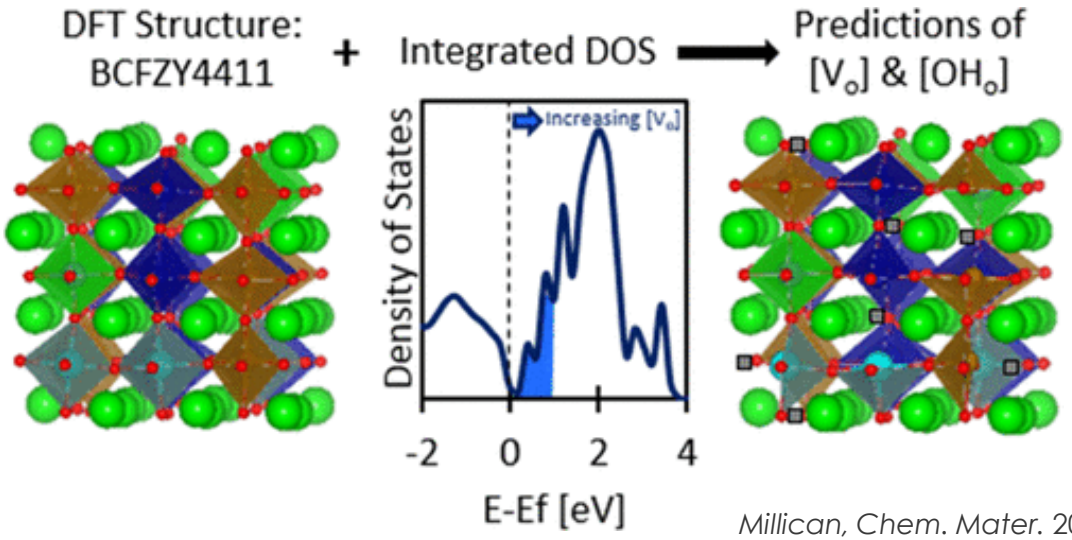

Millican, Chem. Mater. 2022, 34, 2, 510.

Magnetic/Electronic Structures vs. δ

Non-Rigid Band Type Defect Behavior

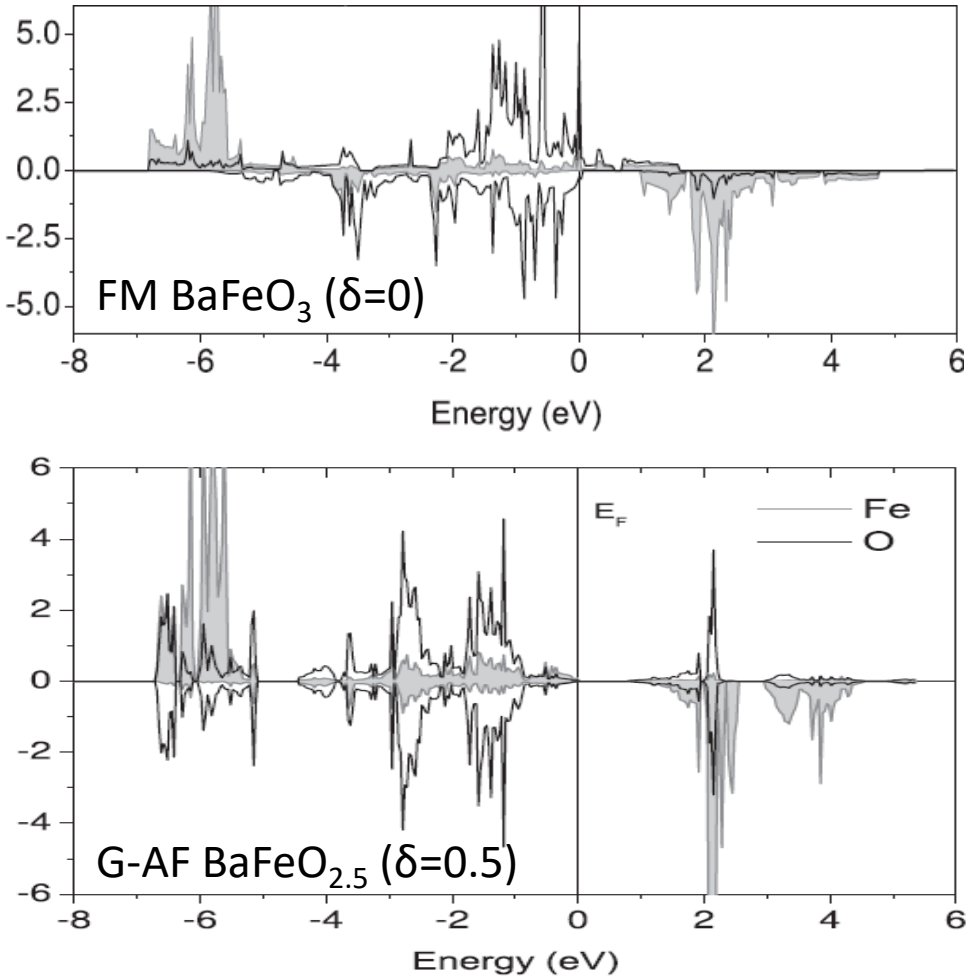

Ribeiro, Journal of Applied Physics 113, 083906 (2013).

$La_{1-x}Sr_xFeO_{3-\delta}$

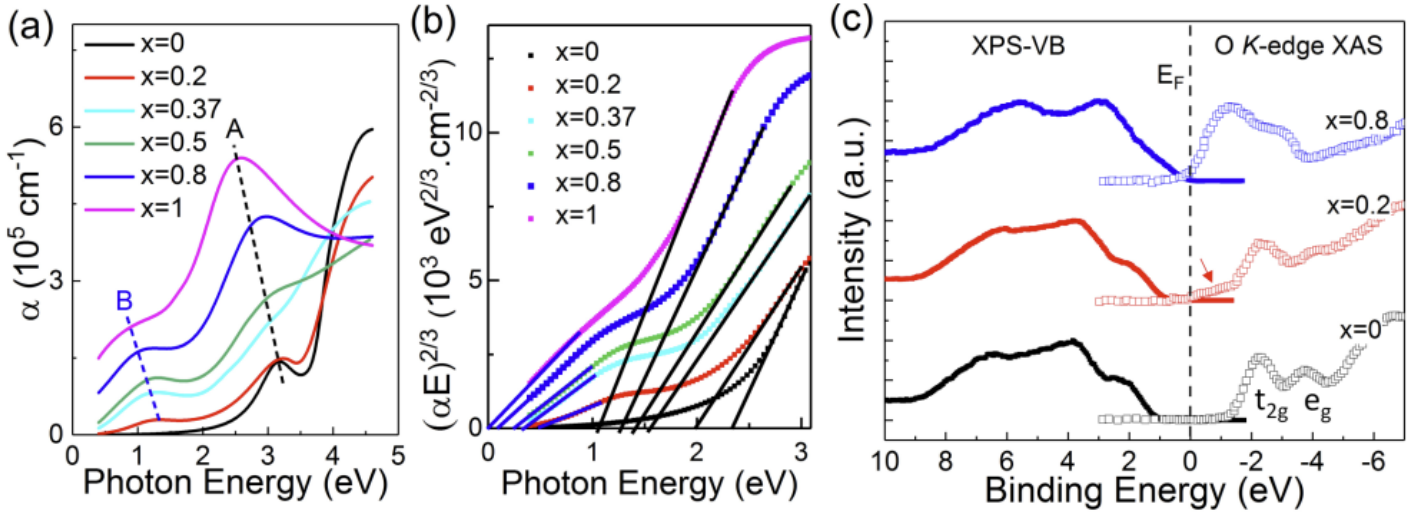

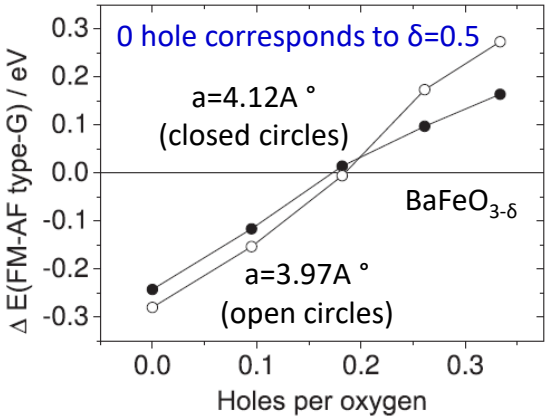

Ribeiro, Journal of Applied Physics 113, 083906 (2013).

- Electronic structures of Fe based perovskites show non-rigid band behavior with increasing hole doping.
- Coupled with magnetic ordering transition vs. δ.

Wang, Phys. Rev. Mater., 2019, 3, 025401.

$BaFeO_{3-\delta}$ Magnetic/Electronic Structures vs. δ and $OH_O^{\bullet}$

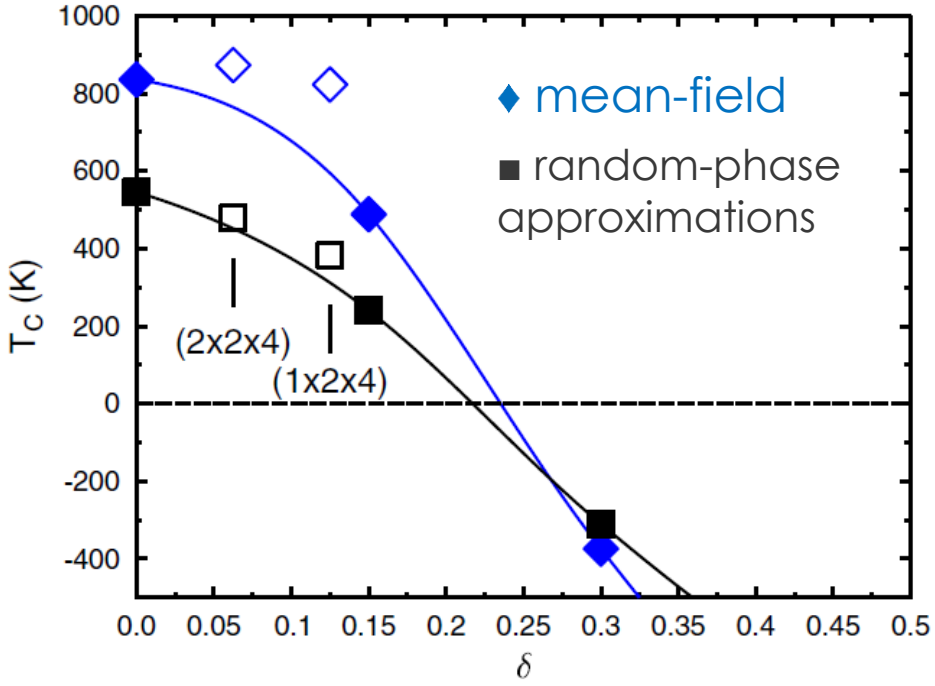

The negative T_C means the absence of ferromagnetic order.

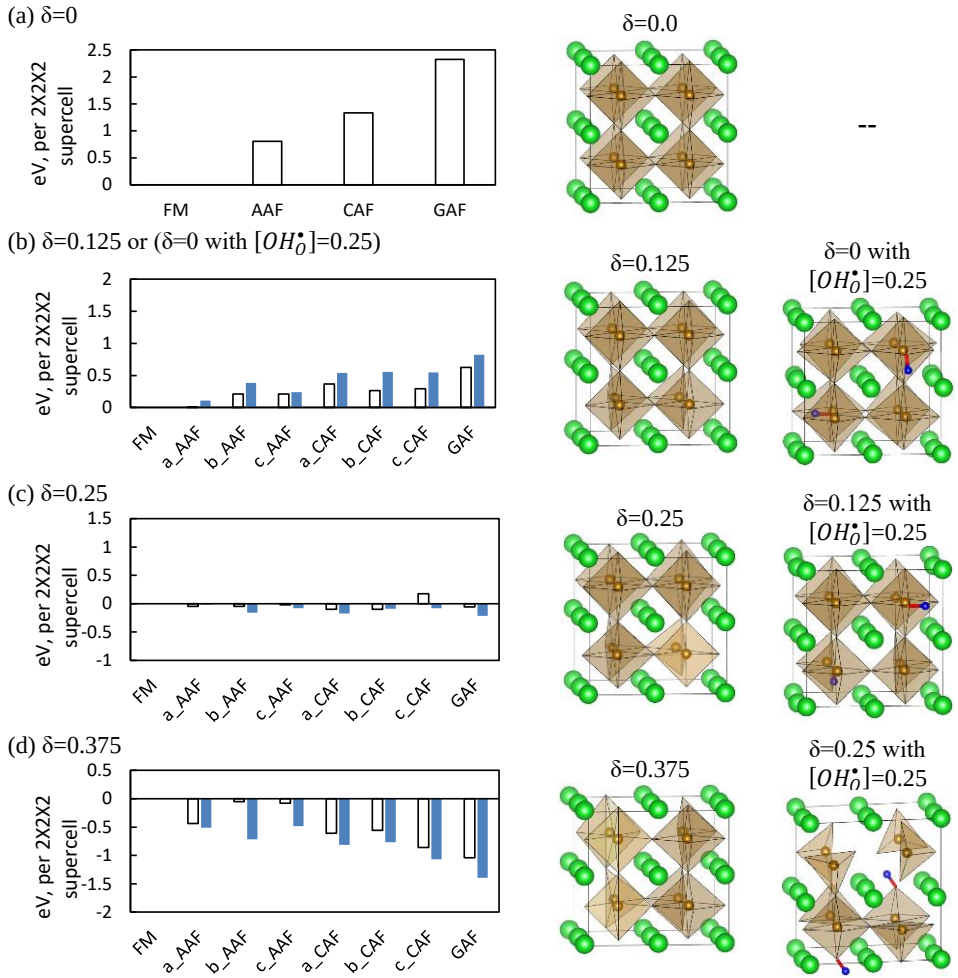

*Maznichenko, Phys. Rev. B, 2016, **93**, 024411.*

ECS Transactions, (2023) 111, (6) 1823-1838.